Acta Cryst. (1981). A**37**, 449–456

Crystal Structure and Charge Carrier Behaviour of $(W_{12\cdot64}Mo_{1\cdot36})O_{41}$ and its Significance to Other Related Compounds

BY K. VISWANATHAN

Mineralogisches Institut der Technischen Universität Braunschweig, Gauss-Strasse 29, *D*-3300 *Braunschweig, Federal Republic of Germany*

AND E. SALJE

Mineralogisches Institut der Technischen Universität Hannover, Welfengarten 1, *D*-3000 *Hannover, Federal Republic of Germany*

(*Received* 6 *August* 1980; *accepted* 13 *October* 1980)

Abstract

The crystal structure of $(W_{12\cdot64}Mo_{1\cdot36})O_{41}$, containing {102} crystallographic shear (*CS*) planes, has been solved. $a = 23\cdot939\,(9)$, $b = 3\cdot966\,(1)$, $c = 16\cdot729\,(15)$ Å, $\beta = 106\cdot74\,(5)°$; $P2/c$; $R = 0\cdot10$ for 1285 reflections. It was shown that the Mo atoms segregate on positions in the *CS* planes. The O atom octahedra are distorted in typical arrangements, so that the elastic strain energy could be estimated. The hypothetical phases $(W,Mo)_nO_{3n-1}$ for a wide range of values of n were derived from the experimental atomic parameters. Optical and electrical experiments show the existence of two types of charge carriers, a minority in the interplanar material, which contribute to conductivity, and a majority of trapped positions in the *CS* planes, preferentially on Mo positions.

Introduction

Substoichiometric compounds of transition-metal oxides tend to form ordered defect structures. In WO_{3-y} and MoO_{3-y} these defects are crystallographic shear (*CS*) planes containing chains of edge-sharing octahedra in a matrix of corner-sharing octahedra. Magnéli (1948) determined their principal structural arrangement. Later electron microscopy showed the existence of *CS* phases in a wide range of chemical systems $(Me,W)O_{3-y}$, where Me = Mn, Fe, Co, Ni, Cr, Mo (*e.g.* Ekström & Tilley, 1977). Unfortunately, the arrays of *CS* planes turned out to be considerably disordered and hence X-ray analysis could only determine the approximate metal positions (Blomberg, Kihlborg & Magnéli, 1953). We overcame this problem by growing crystals of ternary oxides WO_{3-y}–MoO_{3-y} containing highly ordered *CS* planes.

The physical behaviour of these phases is interesting because of the charge compensation mechanism. The substoichiometry of oxygen is compensated by the presence of excess electrons. In contrast to the defects in halide crystals no lattice site vacancies exist to trap these electrons. It was found by Berak & Sienko (1970) that these electrons are localized at random at the metal positions, accompanied by a deformation of the surrounding structure. These so-called polarons react sensitively to changes in crystal structure, temperature, *etc.* (Salje, 1979; Schirmer & Salje, 1980*a*,*b*). In such cases, just *one* electron can be trapped per metal position (W^{5+}) as long as the crystalline state is not destroyed (Salje, Carley & Roberts, 1979). In addition, two such states couple to give rise to bi-polaron formation (Schirmer & Salje, 1980*a*).

When Mo and W are both present in *CS* phases, the trapping probability is much higher for Mo than for W (Salje, Carley & Roberts, 1979). It is therefore possible to locate the five-valent states just by the determination of Mo positions. We reported earlier (Salje, Gehlig & Viswanathan, 1978) that in fully oxidized ternary oxides $W_xMo_{1-x}O_3$ the W and Mo atoms are randomly distributed at the metal positions. Blomberg, Kihlborg & Magnéli (1953) suggested a statistical distribution of Mo and W atoms in $(Mo,W)_{10}O_{29}$. On the other hand, Salje, Carley & Roberts (1979) inferred from the results of ESCA experiments on substoichiometric material some segregation of Mo in the *CS* planes. This paper describes the X-ray structure analysis of $(W_{12\cdot64}Mo_{1\cdot36})O_{41}$.

Optical and electrical conductivity

The experimental methods of reflection spectroscopy and measurements of the specific conductivity have been described (Viswanathan & Salje, 1980). In spectroscopic experiments, powders have been used for back-reflection measurements; the corresponding absorption spectrum was then calculated from the

0567-7394/81/040449-08$01.00

reflectivity data with the Kubelka–Munk formalism. This method has been discussed by Kortüm (1969) and was applied to other W and Mo oxides by Salje & Hoppmann (1980). The resulting absorption spectrum is given in Fig. 1. It shows a single peak at 0·95 eV, the shape of which is similar to those of the polaronic absorption peaks of WO_3 at low temperatures. The absorption curve is in strong contrast to the quasi-metallic behaviour of sodium tungsten bronzes or to WO_3 at room temperature for which a Drude-like profile was found. It must therefore be concluded that all carriers contributing to the optical absorption are localized in shallow traps. The optical density is extremely high according to the theoretical carrier concentration of $2\cdot7 \times 10^{27}$ m^{-3}.

The specific conductivity along the direction of the *CS* planes is 0·7–2 $(\Omega\ \text{mm})^{-1}$ at room temperature with semiconducting behaviour at low temperatures. This value is of the same order of magnitude as the results for WO_3 at room temperature with a corresponding carrier concentration of $3–7 \times 10^{24}$ m^{-3}. Under the assumption that the same carrier mobility holds for WO_3 and $(W_{12\cdot64}Mo_{1\cdot36})O_{41}$ [hereafter shortened to $(Mo,W)_{14}O_{41}$] the resulting concentration of carriers which contribute to the specific conductivity should be the same for the *CS* phases. Hence the optical carrier density is *ca* three orders of magnitude higher than those of the conducting carriers. Consequently, two types of carriers exist in these substoichiometric compounds: (1) quasifree carriers which contribute to the hopping conductivity and (2) the majority of carriers, which are trapped and contribute to the optical absorption but not to the specific conductivity. Structurally, the second set of carriers is localized in the *CS* planes whereas the conducting electrons travel between. The *CS* planes are areas of reduced conductivity in a matrix of semiconducting bulk material.

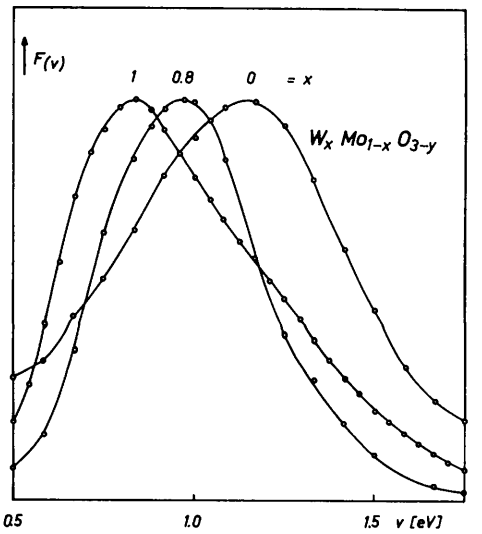

Fig. 1. Kubelka–Munk functions, $F(v)$, of $WO_{2\cdot99}$, $MoO_{2\cdot99}$, and $(Mo,W)_{14}O_{41}$, representing the approximate absorption spectrum. $F(v)$ is normalized with respect to the same peak height for all compounds.

Occurrence of *CS* phases in $W_xMo_{1-x}O_{3-y}$

The structural chemistry of reduced binary oxides WO_{3-y} and MoO_{3-y} is well established. In WO_3 initial reduction leads to the formation of {102} *CS* planes; further reduction to compositions of the order $WO_{2\cdot93}$ produces oxides containing {103} *CS* planes. In addition, tunnel structures occur at $WO_{2\cdot82}$ and $WO_{2\cdot72}$. The structure of the latter has been published (Viswanathan & Salje, 1980).

Reduction of MoO_3 also leads to the formation of *CS* phases (Bursill, 1969, 1972; Kihlborg, 1963). Two of them, Mo_8O_{23} and Mo_9O_{26}, have structures similar to the reduced WO_{3-y} containing ordered {102} *CS* planes. Recent studies on the ternary system $W_xMo_{1-x}O_3$ (Salje, Gehlig & Viswanathan, 1978) reveal that framework structures similar to that of MoO_3 are found only for compositions near to MoO_3.

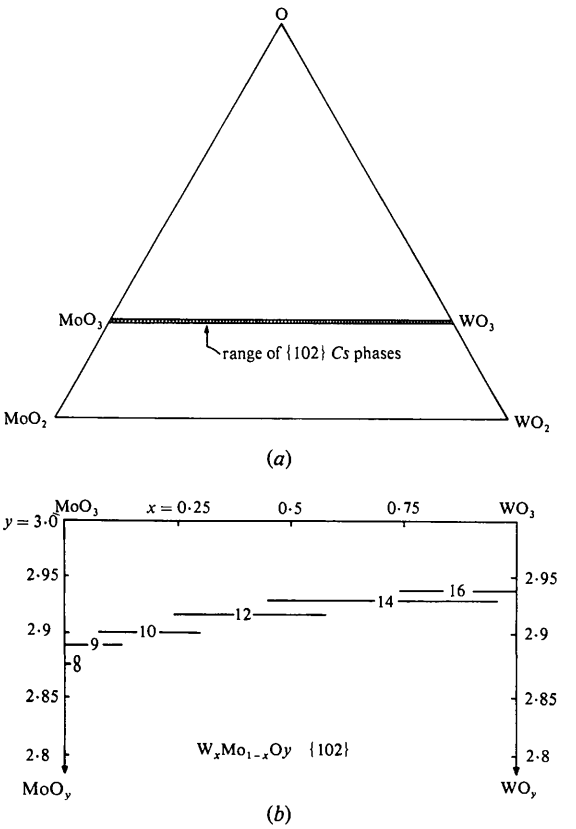

Fig. 2. Tentative diagram of phases containing {102} crystallographic shear planes. (*a*) Phase diagram with stability range of *CS* phases. (*b*) Observed n values of $(W_xMo_{1-x})_nO_{3n-1}$ as a function of the chemical composition. The lines indicate the range of the nominal chemical composition, the n values are inserted.

All other compounds possess structures closely related to the WO_3 type with random distribution of W and Mo at the metal positions (Magnéli, 1953).

The crystal chemistry of the reduced ternary oxides will be published in a separate paper (Ekström, Tilley & Salje, 1981). The present examination was carried out on selected, slightly reduced probes with a JEM 100 B electron microscope fitted with a top-entry goniometer stage and operated at 100 kV. In crystals prepared at temperatures above 983 K the only ternary phases observed to form were of general formula $(W,Mo)_nO_{3n-1}$ with $n = 9$, 10, 12 and 14. These phases

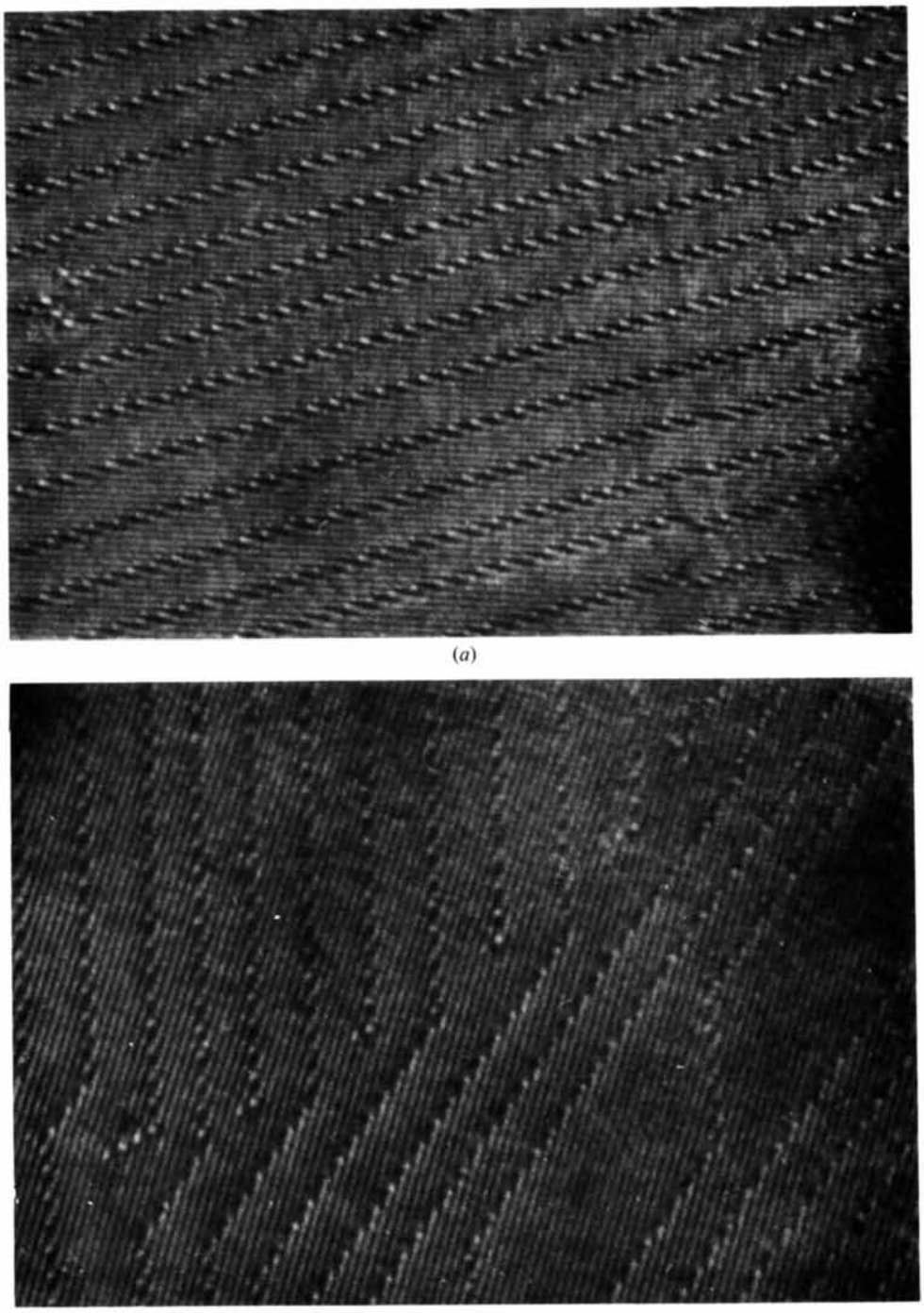

(*a*)

(*b*)

Fig. 3. Two typical types of disorder of the $(W_xMo_{1-x})_nO_{3n-1}$ phases. (*a*) A quasi-continuous variation of the interplanar distances and hence the n values. (*b*) Shear planes of different orientations {102} and n values.

contain {102} *CS* planes. In general those crystals with smallest n value were richest in Mo and showed a highly ordered distribution of *CS* planes. This is in accordance with the observations of Blomberg, Kihlborg & Magnéli (1953) and Magnéli (1953). In all charges crystals of different n values were observed but those with the given n values always predominated. Except for $n = 9$, all other values are even. This effect is similar to the findings for WO_{3-y} (Iguchi & Tilley, 1977). Under the assumption that the most frequently observed n values correspond to equilibrium states, our results can be depicted in a tentative phase diagram (Fig. 2).

To determine the structure, we chose a crystal with $n = 14$ because the spacings between the *CS* planes are large enough to enable a study of the nature of deformation of the octahedra far from the *CS* planes. In Fig. 3 the electron-microscopy pictures of a highly ordered and a disordered phase are given.

Structural analysis

Crystals of $W_{14}O_{41}$, found to be highly ordered by electron microscopy, were examined with a precession camera. One crystal, whose precession photographs revealed minimum diffuseness of reflections, was chosen for the structure determination.

The exact composition of the crystal is $(W_{12\cdot64}Mo_{1\cdot36})O_{41}$. The lattice constants determined with an automatic diffractometer are $a = 23\cdot939$ (9), $b = 3\cdot966$ (1), $c = 16\cdot729$ (15) Å, $\beta = 106\cdot74$ (5)° (space group $P2/c$). The intensities were collected on a Stoe four-circle automatic diffractometer with Mo $K\alpha$ radiation and a graphite monochromator. 4001 reflections were measured in the 2θ range 0–50°, and were reduced to 2201 symmetry-independent reflections. Of these only about 705 reflections could not be considered weak because their intensities were larger than 5% of that of the strongest reflection. Of the weak reflections, those with $F < 2\sigma(F)$ were not included in the refinement. As a result only 1285 reflections could be used for final refinement.

The crystals of $(Mo,W)_{14}O_{41}$ are thin plates, in contrast to the needle-shaped crystals of $(Mo,W)_{10}O_{29}$ and $(Mo,W)_{11}O_{32}$ (Blomberg, Kihlborg & Magnéli, 1953). These plates are parallel to (100) and are also parallel to the *CS* planes (Fig. 4). The crystal used for structure determination is one such plate of irregular shape. Hence for calculating the absorption correction, the crystals could not be described very accurately. However, this was not considered a serious handicap because, as the structural principles are known, the approximate parameters of the metal positions could be inferred and used for a preliminary refinement. This revealed small discrepancies in the structure factors of strong reflections, which were found to depend upon their calculated transparencies. Then the reflections were divided into ten groups on the basis of their calculated transparencies and each group was provided with a separate scale factor. A subsequent refinement of the scale factors not only led to a drop in R, but also showed an unequivocal, approximately linear, correlation between the scale factors and the calculated transparencies.

After determining the metal positions by least-squares refinement, the O atom positions were determined from difference syntheses. R arrived at with isotropic temperature factors is 0·11. Refinement with isotropic temperature factors was stopped when two oxygen parameters became negative. Anisotropic temperature factors were then refined only for the heavier metal atoms. The final R for all 1285 reflections is 0·10 (R for the 705 strong reflections is 0·069). The final atomic parameters and important interatomic distances are given in Table 1. The structure is shown in Fig. 4.*

Discussion of the structural deformation

The results of the structure analysis show that no tilts of the octahedra occur. This is in contrast to the structure of all fully oxidized ternary oxides at room temperature (Salje, Gehlig & Viswanathan, 1978). In WO_3 this type of distortion seems to stabilize the structure and hence, from a structural point of view, the linkage of the WO_6 octahedra between the *CS* planes is not similar to that of WO_3.

It is noteworthy that Mo segregates in the *CS* planes at the metal positions 5 and 5′ (Fig. 4), which are related by the inversion center at $(\frac{1}{2},0,\frac{1}{2})$. As we know from ESCA experiments that Mo traps the free electrons more easily than W by forming five-valent states, we conclude that the majority of charge carriers

* Lists of structure factors and anisotropic thermal parameters have been deposited with the British Library Lending Division as Supplementary Publication No. SUP 35740 (26 pp.). Copies may be obtained through The Executive Secretary, International Union of Crystallography, 5 Abbey Square, Chester CH1 2HU, England.

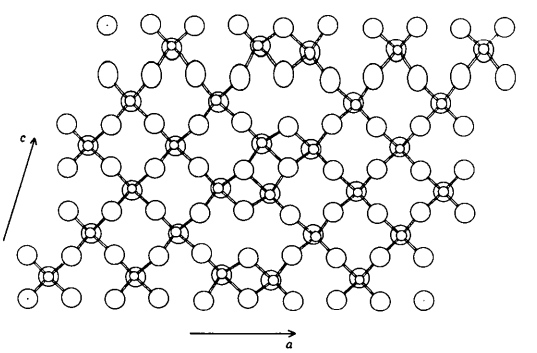

Fig. 4. Crystal structure of $(W_{12\cdot64}Mo_{1\cdot36})O_{41}$.

Table 1. *Atomic parameters and important interatomic distances* (Å)

Standard errors in tungsten parameters: x and z ±0·0002, y ±0·001; and in oxygen parameters: x and z ±0·001, y ±0·005.

	x	y	z
W(1)	0·1072	0·090	0·2477
W(2)	0·3220	0·087	0·2423
W(3)	0·0352	−0·070	0·4157
W(4)	0·2503	−0·070	0·4110
W(5)*	0·4696	0·080	0·4005
W(6)	0·6050	−0·067	0·4249
W(7)	0·8218	−0·070	0·4215
O(1)	0·000	0·000	0·500
O(2)	0·077	0·020	0·337
O(3)	0·184	−0·025	0·330
O(4)	0·297	0·002	0·335
O(5)	0·403	0·010	0·323
O(6)	0·523	0·025	0·340
O(7)	0·632	0·007	0·330
O(8)	0·745	0·030	0·339
O(9)	0·855	0·002	0·335
O(10)	0·965	0·005	0·334
O(11)	0·108	0·007	0·495
O(12)	0·220	0·017	0·500
O(13)	0·329	0·027	0·495
O(14)	0·445	−0·015	0·505
O(15)	0·110	0·530	0·250
O(16)	0·330	0·570	0·250
O(17)	0·035	0·490	0·415
O(18)	0·255	0·450	0·415
O(19)	0·470	0·560	0·405
O(20)	0·598	0·489	0·425
O(21)	0·820	0·450	0·415

W(5)–W(5′) = 3·288 (4), W(5)–W(6) = 3·200 (5)

O(6)–O(6′) = 2·90 (2)

* W(5) position contains $W_{0.56}Mo_{0.44}$.

are localized at the positions 5 and 5′. These two positions are direct neighbours, so that a clustering of two five-valent states, similar to the bi-polaron formation, occurs in the *CS* planes. The charge carrier distribution in the *CS* planes is therefore by no means uniform nor do W^{4+} states appear (Iguchi & Tilley, 1977).

The segregation of Mo explains the relatively low conductivity in spite of the high carrier density. It seems that in all *CS* phases the conductivity is governed by electrons of two different types. Most of the charge carriers are trapped in the *CS* planes, in our case by Mo at position 5 and 5′. A tunnelling to the equivalent positions in the next Me_4O_{11} block is not possible because the occupancy probability of Mo of the next position is also very high and the Mo–Mo distance is rather large (>6·0 Å). This means that the *CS* planes are regions of low conductivity. In the regions between the *CS* planes a certain number of carriers must also be expected because five-valent states were found to a certain degree at the W positions (Salje, Carley & Roberts, 1979). The carrier mobility is for structural reasons not too different from that of WO_3 and consequently the carrier concentration must be of the same order of magnitude as in synthetic WO_3 crystals, say *ca* 10^{25} m^{-3}. Just these carriers dominate the electrical conductivity and *not* the *ca* 10^{27} m^{-3} carriers in the *CS* planes. However, the optical density is preferentially determined by the localization of the Mo^{5+} in the *CS* planes.

The geometrical distortion of the crystal structure exhibits three outstanding features:

(*a*) the large distance between O(6) and O(6′) [2·90 (2) Å]: These two O atoms (Fig. 4) are not shielded by metals and hence the repulsive interaction enhances their distance. Although it is known that the Coulomb interaction is rather small in WO_3 (Salje, 1976), we assume the ionic part to be of sufficient strength to cause this deformation.

(*b*) the off-centering of the metal positions in the **b** direction: This displacement of Mo and W atoms follows a zig-zag pattern along the fourteen corner-sharing octahedra which determine the superstructure. These chains are linked together in the *CS* planes with the two outer octahedra, which have just one corner-sharing neighbour, in which the metal atoms follow the zig-zag movement as end members of the chains. The W atoms in the two inner octahedra (5 and 5′ in Fig. 4) are, in turn, displaced in opposite directions with respect to the metal atoms in both the neighbouring corner-shared octahedra respectively.

(*c*) the off-centering of the metal positions in the *ac* planes: The metal positions in the *CS* plane are shifted from the midpoints of the octahedra so as to increase the distances between them. The W atoms in the octahedra which are directly linked with the *CS* planes have moved away from the *CS* planes. Let us call this layer α. The next layer β is not directly linked with the octahedra in the *CS* planes. They show reduced off-centering of W. The third layer γ is in the central region between the two *CS* planes and reveals practically no off-centering.

Discussion of the phase stability

The lattice constants given in this paper differ slightly from those of Magnéli, Blomberg-Hansson, Kihlborg & Sundkvist (1955) for $(W_{0.48}Mo_{0.52})_{14}O_{41}$. This shows that the lattice parameters depend on the Mo content and on the n value. In crystals with low Mo content Mo is segregated in the *CS* planes. With increasing Mo content, it enters the other metal positions and causes an increase in b.

It has been widely discussed why the *CS* planes do not approach each other too closely, say $n < 8$. As a major argument, an increase of the elastic strain energy with decreasing distances between the *CS* planes was proposed by Iguchi & Tilley (1977). From the

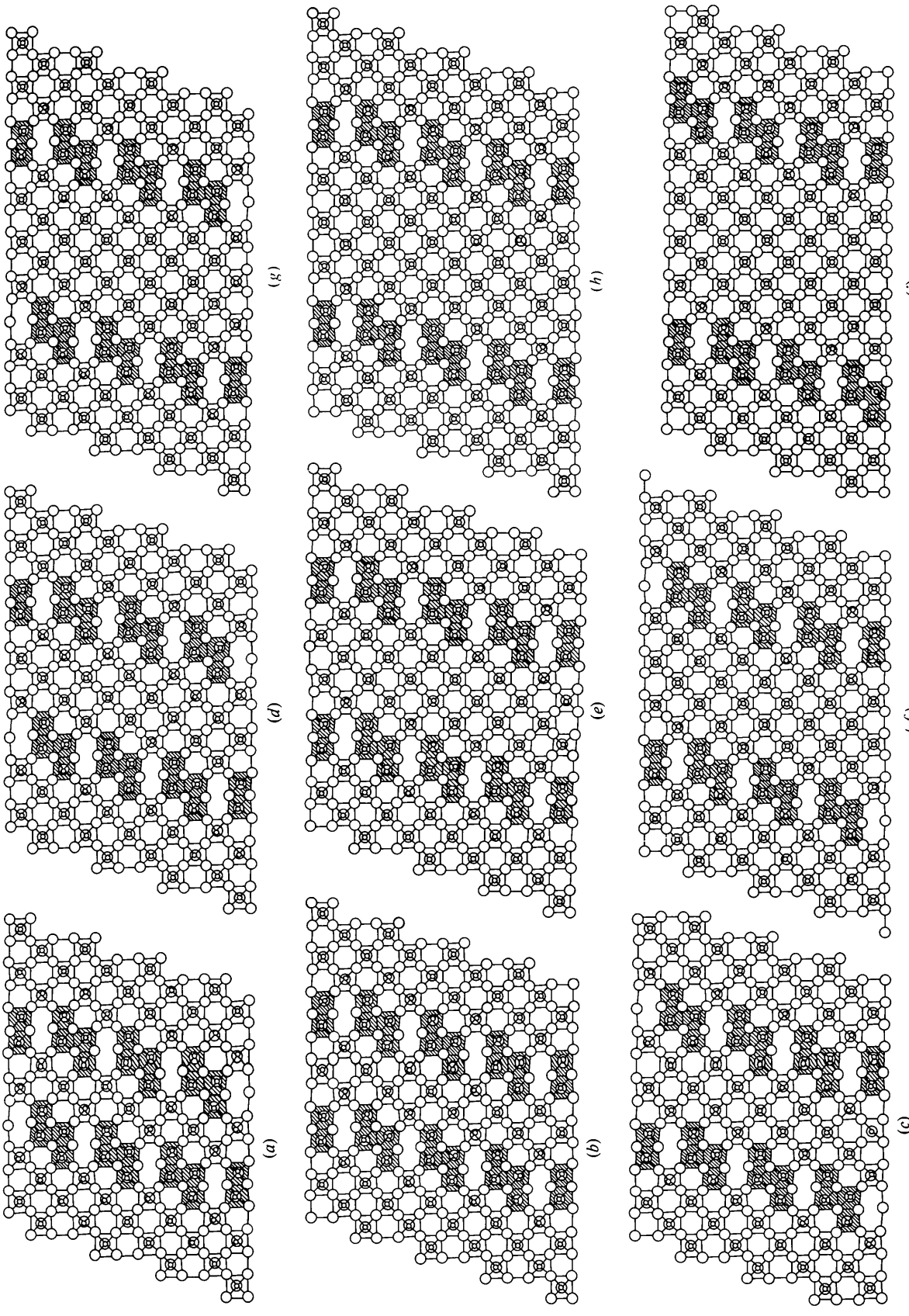

Fig. 5. Hypothetical structures $(W,Mo)_nO_{3n-1}$ with different n values derived from the structural parameters of $(W,Mo)_{14}O_{41}$. (*a*) $n = 7$, (*b*) $n = 8$, (*c*) $n = 9$, (*d*) $n = 10$, (*e*) $n = 11$, (*f*) $n = 12$, (*g*) $n = 13$, (*h*) $n = 14$, (*i*) $n = 16$.

structural parameters, the elastic strains can be classified qualitatively as follows:

(*a*) The intraplanar strains due to the repulsion of the unshielded O atom pairs and due to metal off-centering.

(*b*) The interplanar strains caused by the presence of shear planes on the octahedra in the layers α, β and γ. These strains decrease with the distance away from the *CS* planes, as judged from distortion of the respective octahedra. The octahedra in α are characterized by considerable off-centering of W away from the *CS* plane. Moreover, every second octahedron in an α layer is linked directly to an octahedron in the *CS* plane, in which the displacement of the metal atom along **b** is in the same direction, thereby increasing the strain energy. These deformations are clearly of short-range character and are directly correlated with the linkage of corner-sharing octahedra with the layer α. Because of the predominantly short-range character of these stress interactions, we assume that these deformations are the same for all {102} *CS* phases. We can therefore construct theoretical structural patterns of all phases by juxtaposition of the different layers α, β and γ.

The results are given in Fig. 5. The corresponding calculated lattice constants are listed in Table 2. The *b* lattice constants do not depend on this arrangement and are taken from Magnéli, Blomberg-Hansson, Kihlborg & Sundkvist (1955), with whose data the other lattice constants agree well.

The elastic strain energy can now be estimated. The elastic strains in the *CS* planes are the same for all planes and do not depend on the *n* value. Hence they were omitted, as we are interested only in the relative elastic energies and not in the absolute ones.

The bulk strains due to the formation of the *CS* planes are proportional to the number of octahedra α, β and γ per unit volume. These numbers are given in Table 2 and the density of the α, β and γ octahedra per unit volume are plotted in Fig. 6. It appears that, with decreasing *n* value, the elastic strain energy, which can be considered proportional to the density of the different octahedra, increases rapidly and for *n* values below $n \simeq 7$ it becomes unrealistic.

Another factor for the enhanced stability of certain *CS* phases is the geometrical arrangement of α, β and γ octahedral sheets relative to each other. In Table 2 the number of the different types are given; their mutual arrangements are shown in Fig. 5. A best fit of these sheets is found for the combinations $n_\alpha = n_\beta = n_\gamma$; $n_\alpha = n_\beta$, $n_\gamma = 0$; $n_\alpha \neq 0$, $n_\beta = n_\gamma = 0$. A comparably equivalent fit is given if just one half of a sheet is occupied, *e.g.* $n_\alpha = n_\beta = 8$, $n_\gamma = 4$ in $Me_{14}O_{41}$. Accordingly, the most stable phases are $n = 8$, $n = 10$, $n = 12$, $n = 14$ and $n = 16$. In fact, exactly these phases besides $n = 9$ have been found to occur more frequently than others (Magnéli, Blomberg-Hansson, Kihlborg & Sundkvist, 1955; this paper). The stability of $n = 9$, probably dominating $n = 8$, can be explained by the fact that in the $n = 8$ arrangement, α octahedra are directly linked without any stress-reducing β octahedra between them. The $n = 9$ phase is the one with the smallest distance between the *CS* planes but with additional β octahedra between the heavily deformed octahedra of type α.

In conclusion, we explain the fact that *CS* phases with shorter distances than those in $n \simeq 7$ have not

Table 2. *Calculated lattice constants and number of distorted octahedra of type* α, β *and* γ *for different n values*

n	*a* (Å)	*b* (Å)	*c* (Å)	β' (°)	α	β	γ
7	16·72	4·06	13·81	124	6	0	0
8	16·72	4·052	13·40	73·5	8	0	0
9	16·72	4·027	14·62	95·4	8	2	0
10	16·72	4·005	17·45	111·7	8	4	0
11	16·72	4·00	18·76	73·7	8	6	0
12	16·72	3·956	19·60	89·3	8	8	0
13	16·72	3·96	21·80	102·5	8	8	2
14*	16·729	3·966	23·939	73·26	8	8	4
15	16·72	3·96	24·22	94·5	8	8	6
16	16·72	3·94	26·50	96·5	8	8	8

* *a* and *c* have been interchanged for comparison with other results.

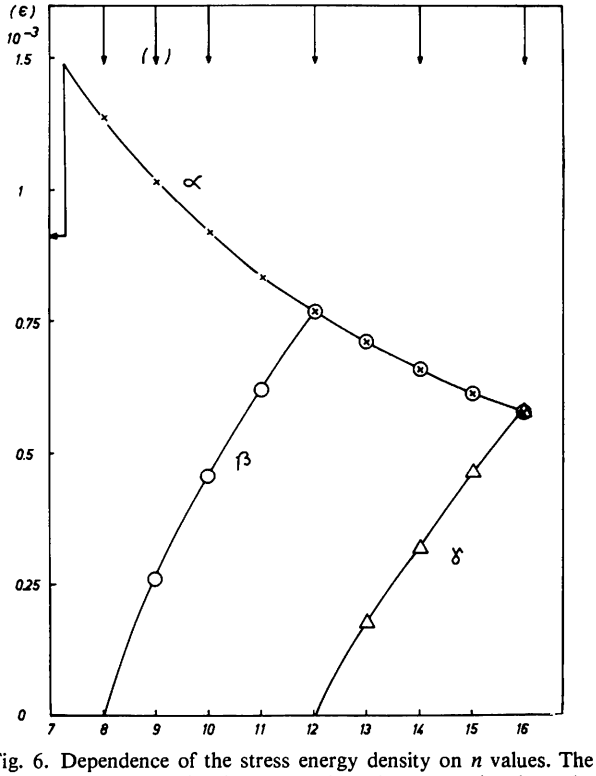

Fig. 6. Dependence of the stress energy density on *n* values. The stress energy density is proposed to be proportional to the density of octahedra of type α, β and γ. The stable phases are indicated by arrows.

been observed because of the enormous increase of the elastic strain energy due to the higher density of α octahedra. Instead, phases with {103} *CS* planes, but with larger n values, are expected to form. Moreover, phases with $n = 8, 9, 10, 12, 14$ and 16 are more stable than others because of the better fit between the octahedra of the different layers.

The financial support of Deutsche Forschungsgemeinschaft (Grant Vi 66) is gratefully acknowledged. Thanks are also due to Dr R. J. D. Tilley for help in the electron-microscopic investigations and for fruitful discussions. We are also indebted to Mr K. Brandt for collecting data on the precession camera and automatic diffractometer.

References

BERAK, J. M. & SIENKO, M. J. (1970). *J. Solid State Chem.* **2**, 109–133.
BLOMBERG, B., KIHLBORG, L. & MAGNÉLI, A. (1953). *Ark. Kemi*, **6**, 133–138.
BURSILL, L. A. (1969). *Proc. R. Soc. London Ser. A*, **311**, 267–290.
BURSILL, L. A. (1972). *Acta Cryst.* A**28**, 187–191.
EKSTRÖM, T. & TILLEY, R. J. D. (1977). *J. Solid State Chem.* **22**, 331–340.
EKSTRÖM, T., TILLEY, R. J. D. & SALJE, E. (1981). In preparation.
IGUCHI, E. & TILLEY, R. J. D. (1977). *Philos. Trans. R. Soc. London*, **286**, 55–85.
KIHLBORG, L. (1963). *Ark. Kemi*, **21**, 471–495.
KORTÜM, C. (1969). *Reflexionsspektroskopie.* Berlin: Springer.
MAGNÉLI, A. (1968). *Acta Chem. Scand.* **2**, 501–517.
MAGNÉLI, A. (1953). *Acta Cryst.* **6**, 495–500.
MAGNÉLI, A., BLOMBERG-HANSSON, B., KIHLBORG, L. & SUNDKVIST, G. (1955). *Acta Scand.* **9**, 1382–1390.
SALJE, E. (1976). *Acta Cryst.* A**32**, 233–238.
SALJE, E. (1979). *Opt. Commun.* **24**, 231–232.
SALJE, E., CARLEY, A. F. & ROBERTS, M. W. (1979). *J. Solid State Chem.* **29**, 237–251.
SALJE, E., GEHLIG, R. & VISWANATHAN, K. (1978). *J. Solid State Chem.* **25**, 239–250.
SALJE, E. & HOPPMANN, G. (1980). *Philos. Mag.* In the press.
SCHIRMER, O. F. & SALJE, E. (1980*a*). *Solid State Commun.* **33**, 333–336.
SCHIRMER, O. F. & SALJE, E. (1980*b*). *Phys. Rev. Lett.* In the press.
VISWANATHAN, K. & SALJE, E. (1980). *J. Solid State Chem.* In the press.

Acta Cryst. (1981). A**37**, 456–459

The Influence of Systematic Errors in Crystal Structure Refinements Using Guinier Camera X-ray Intensity Data

BY H. G. SCOTT

CSIRO Division of Materials Science, Engineering Ceramics and Refractories Laboratory, PO Box 4331, *Melbourne, Victoria* 3001, *Australia*

(*Received* 26 *November* 1980; *accepted* 5 *January* 1981)

Abstract

The effect of systematic errors on the reliability of crystal structure refinements based on Guinier camera powder data has been investigated. Three structures were refined with Guinier integrated intensity data, and the results are compared with published single-crystal determinations. In each case, the effect of systematic errors could be adequately corrected by an overall temperature factor, though in one case a significant decrease in the residual resulted from the inclusion of an idealized specimen absorption correction. Atomic temperature factors determined from the Guinier data were highly correlated with the correction terms: atomic coordinates were insensitive to the corrections, and agreed well with the corresponding single-crystal values.

Introduction

Structure determination from powder data has been stimulated by the development of the profile refinement technique (Rietveld, 1967, 1969). Applied originally to neutron diffraction data, it has been extended to Guinier camera X-ray powder data by Malmros & Thomas (1977). The technique reduces the problem of overlapping of non-equivalent reflexions, common in powder data, but there is some doubt as to whether current profile refinement programs estimate the stan-

0567-7394/81/040456-04$01.00